Universal behavior of the amplitude ratio of percolation susceptibilities for off-lattice percolation models

Sang Bub Lee
Department of Physics, Kyungpook National University, Taegu 702-701 Korea
(Received 13 November 1995)

We study the amplitude ratio of percolation susceptibilities, $R = C_-/C_+$ (C_- and C_+ being the amplitudes below and above the percolation threshold), which is supposed to be universal but has been found to be different for certain continuum models from that of the ordinary lattice percolation. We specifically consider two off-lattice percolation models, the continuum percolation of the penetrable-concentric-shell model and the randomly bonded percolation model, for both of which R was found to be different from the lattice value while various critical exponents remain the same. By numerical investigation we find that R depends on the size of the system for both models; after a finite-size effect is carefully taken into account, R is consistent with the lattice value, indicating a strong universality between lattice and off-lattice percolation models. We also discuss some subtleties of the finite-size scaling analyses.

PACS number(s): 05.20.−y, 05.70.Fh, 64.60.Ak, 64.60.Fr

I. INTRODUCTION

Percolation models have served well as theoretical tools to investigate many interesting physical phenomena. Example phenomena include the transport, mechanical, and electromagnetic properties of disordered media [1–3]. The simplest percolation model is ordinary lattice (site) percolation, in which each lattice site is either occupied with probability p or unoccupied with probability $1 - p$; any two occupied neighbor sites are assumed to be connected and belong to the same cluster. The statistical properties of this simple model have been investigated during the past several decades and a large amount of information is now available [1]. However, for real physical systems, the off-lattice or continuum percolation models are more appropriate since they are morphologically more analogous to the real systems than their lattice counterparts. (In what follows, we will use the term "continuum" in contrast to "lattice," i.e., all off-lattice models are assumed to be continuum models.) The polyfunctional condensation of monomers, hydrogen bond networks in liquid water, crosslinking of polymers, and two-composite disordered media are such examples.

The universality of continuum percolation models has been investigated by many authors via Monte Carlo simulations [4,5], molecular dynamics calculations [6,7] and Monte Carlo renormalization studies [8–10]. The universal critical exponents ν, γ, and β were found to be consistent with the corresponding lattice values, suggesting that the lattice and continuum models belong to the same universality class. Here ν, γ, and β characterize, respectively, the correlation length, the mean cluster size (often called the susceptibility), and the order parameter near the critical point p_c at which a geometrical phase transition from a nonpercolating phase to a percolating phase takes place.

However, it has also been reported that the amplitude ratio of susceptibilities (defined by $R = C_-/C_+$, where C_- and C_+ are the amplitudes below and above p_c, respectively), which is supposed to be universal [11], is at least one order of magnitude smaller than the lattice value for certain models of continuum percolation. Typical examples include the off-lattice model of randomly bonded percolation (RBP) [12], continuum percolation of overlapping spheres, capped cylinders, and widthless sticks [13]. On the other hand, for continuum percolation of penetrable-concentric-shell (PCS) models [14], R was found to be considerably larger than the lattice value [15,10]. These unusual results lead us to speculate that lattice and continuum percolations are in different universality classes and/or R is not universal for continuum percolation models.

In contrast, results that are different from those described above were also reported for certain models of continuum percolation. The present author carried out extensive Monte Carlo simulations in two and three dimensions for the continuum percolation of overlapping disks and spheres and of the PCS model [15]. The amplitude ratios for the former models were found to be close to the lattice values, while for the PCS model considerably larger values were still observed. Frith and Buscall [7] also studied, using molecular dynamics calculations, the percolation of hard spheres and found that the amplitude ratio R, as well as the exponents ν and γ, was similar to the lattice values. Considering these results, it is still unclear whether or not R is universal for all continuum models.

All these works were carried out on relatively small-size systems and did not include careful discussions of the finite-size effect. We, however, claim that the system size significantly affects the estimates of R; thus it is not fair to conclude, without considering the size effect, that R is different from the lattice value. In this work, we present extensive Monte Carlo results for R, carefully analyzed

with respect to finite-size, for two typical models in which the values of R were previously found to be different from the lattice values. We found that the estimates of R vary significantly depending on the size L of the system and, after extrapolating the results as $L \to \infty$, the values of R appear to be similar to the lattice values.

The models we consider in this work are the continuum percolation of the PCS model and the RBP model. In the PCS model, each sphere of radius $\sigma/2$ is composed of an impenetrable core of radius $\lambda\sigma/2$, enclosed by a perfectly penetrable shell of thickness $(1-\lambda)\sigma/2$. The extreme limits of $\lambda = 0$ and 1 correspond, respectively, to the cases of fully penetrable and totally impenetrable particles. The number density ρ or, equivalently, the reduced number density $\eta = \rho V_1$ (V_1 being the volume of each particle) can be considered as a control parameter for percolation p. (We prefer to use η since it is dimensionless.) In the RBP model, on the other hand, a predetermined number of particles are distributed randomly in a given system of size L and the bond between two points separated by a distance r is assumed to exist with probability $p(r) = pe^{-r^2/\mu}$, where μ is some constant.

These two models, however, are not unrelated to the lattice percolation model. For example, if we modify the lattice percolation model so that each lattice site can be located on a randomly chosen position in a given system and assume that two sites are connected if their separation distance is less than σ, then the given lattice model would be identical to the model of the fully penetrable spheres of diameter σ. In addition, if we impose a constraint that any two sites cannot be located within a distance of $\lambda\sigma$, we have a PCS model. The fully penetrable particle models can also be reduced to the RBP model if the bonding rule is modified so that the bond exists between two particle centers with probability given by the RBP model. Since the constraints given in these models are all short ranged, one can reasonably expect that they are irrelevant and thus all these models belong to the same universality class. Various critical exponents estimated for these models support this speculation, although the values of R previously reported varied.

This paper is organized as follows. In Sec. II we present the Monte Carlo algorithms for obtaining equilibrium realizations and discuss some subtleties regarding finite-size effects. In Sec. III we present our Monte Carlo results for R including various analyses using finite-size scaling. Section V is devoted to the summary and conclusions.

II. MONTE CARLO PROCEDURES

In this section we present the computer simulation algorithms for obtaining the percolation realizations for the PCS and the RBP models. In the first subsection, we describe the Monte Carlo method we employed to sample the equilibrium realizations and, in the second subsection, we discuss some possible sources of errors occurring in the estimation of R and propose efficient ways to reduce the finite-size effect.

A. Monte Carlo algorithm for equilibrium realizations

There are typically two different methods of obtaining percolation realizations for the PCS model: random sequential addition (RSA) and the Metropolis algorithm [16]. The realizations obtained from both methods are known to exhibit many interesting statistical properties. In the RSA method, particles are added sequentially to randomly chosen positions. When the hard core of each particle is overlapped with that of the previously added particle, the current attempt is discarded and a new position is selected. This procedure is repeated until the desired density is achieved. The realizations obtained in this way are known to exhibit statistical properties quite different from those generated by the Metropolis algorithm. For example, the close-packed volume fraction of hard cores by the RSA method is much lower than that from the Metropolis algorithm. In addition, the realizations obtained by the RSA method are known to be nonequilibrium, while the Metropolis algorithm results in equilibrium realizations. In this work, we employ the Metropolis algorithm to investigate the equilibrium properties.

In the Metropolis algorithm, particles are initially placed in a cubical cell of volume $V = L^d$ on the sites of a regular array (triangular and body-centered arrays for two and three dimensions, respectively). Each particle is then moved by a small displacement to its new position, which is accepted or rejected according to whether or not the inner hard cores are overlapped. When the particle moves out of the cell, we assume that it reenters from the opposite edge. In order to equilibrate, each particle was moved 200 times before beginning to sample the realization. The realizations were selected at an interval of 50–100 moves per particle depending on the concentrations.

In order to sample the susceptibility, one must distinguish various clusters in a system. By definition, two particles are "directly" connected if their interparticle distance is less than the diameter of each particle σ (we set $\sigma = 1$). Pairs of particles may be connected *indirectly* through chains of other particles. In order to find various clusters, we use a standard cluster labeling algorithm (known as the Hoshen-Kopelman algorithm) [17]. For the sake of comparison, we employ both periodic and free boundary conditions. The susceptibility is then calculated according to the definition [to be defined in Eq. (1)].

For the RBP model, a predetermined number of particles $N = \rho L^d$ are distributed randomly in a given system of volume V $(= L^d)$. Each pair of particles is then tested to see if they are directly connected according to the rule defined by the model and the cluster labeling algorithm is employed to analyze the cluster size distribution. The susceptibilities are calculated in a way similar to the PCS model.

B. Finite-size effect

In this subsection, we discuss some possible ways of reducing the errors in R resulting from finite-size effects

occurring in Monte Carlo simulation.

1. Mean cluster size versus susceptibility

The percolation quantity corresponding to the ferromagnetic susceptibility is often defined in two ways:

$$\chi = \sum_s{}' \, n_s s^2 \tag{1}$$

and

$$S = \sum_s{}' \, n_s s^2 \Big/ \sum_s{}' \, n_s s, \tag{2}$$

where n_s denotes the mean number of clusters of size s per site and the prime implies that the spanning cluster is excluded in the sum. The former is usually called the "susceptibility" and the latter the "mean cluster size." In the extreme limit of an infinite system, χ and S are expected to exhibit the same critical behavior near p_c

$$\chi(S) \propto \begin{cases} C_-(p_c - p)^{-\gamma} & \text{for } p < p_c \\ C_+(p - p_c)^{-\gamma'} & \text{for } p > p_c \ , \end{cases} \tag{3}$$

with $\gamma = \gamma'$. While analytically γ and R are defined for the infinite system, the Monte Carlo simulation always deals with a finite system. For any finite system, however, the two definitions in Eqs. (1) and (2) yield different behaviors. This point was discussed in Ref. [18] for lattice model and in Ref. [15] for continuum models and, from both studies, it has been suggested that Eq. (1) should be employed to observe correct asymptotic behavior.

2. Exclusion of the spanning cluster

As the prime denotes in Eqs. (1) and (2), one should exclude the spanning cluster from sampled realizations. In a *real* infinite system, the spanning cluster exists only above p_c and thus should be excluded in the sum for $p > p_c$. However, for any finite system, since the spanning cluster does not always exist even for $p > p_c$ and since p_c is not known accurately for most off-lattice models, researchers have excluded the largest cluster both below and above p_c, assuming that the largest cluster below p_c, is sufficiently small and exclusion of it does not cause significant errors in χ. This approximation apparently underestimates the susceptibility below p_c. To see this clearly, we have calculated the susceptibilities both with and without excluding the largest cluster below p_c, while always excluding it above p_c. We assume that the largest cluster above p_c is part of the spanning cluster even when no cluster spans the cell. Figure 1 shows the susceptibility for the two-dimensional (2D) PCS model with $\lambda = 0.8$ and $L = 150$, obtained using the periodic boundary condition: the closed symbols are the data obtained with the largest cluster below p_c and the open symbols without the largest cluster. The dotted line in (a) indicates the percolation point in the $L \to \infty$ limit, $p_c = 0.7533$ [10]. Clearly

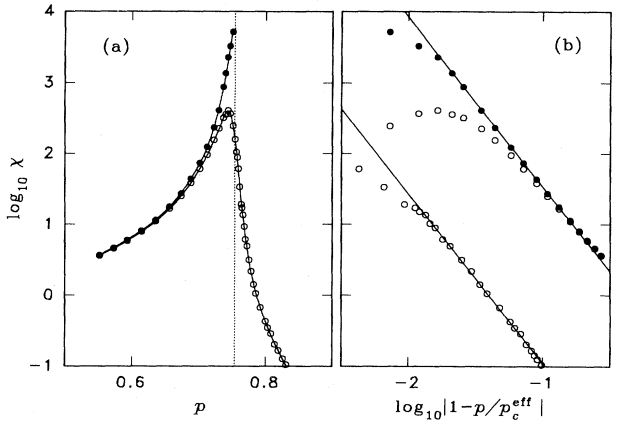

FIG. 1. Monte Carlo data of χ for the PCS model for $\lambda = 0.8$ and $L = 150$, obtained with and without excluding the largest clusters for $p < p_c$, plotted (a) on a semilogarithmic scale and (b) on a double-logarithmic scale with power-law fits. The open symbols are obtained with the largest cluster excluded, while the closed symbols without excluding the largest cluster.

the two sets of data are very different, particularly near p_c, where an asymptotic power law in Eq. (3) is expected to hold. This value of p_c does not, in general, yield the same power law below and above it for a finite system. For any given size of system, one usually treats p_c as a parameter and selects the effective value $p_c^{\rm eff}$, which yields the same power law below and above. Figure 1(b) shows a double logarithmic plot of χ against $|1 - p/p_c^{\rm eff}|$. The solid lines are the best fit to the data without excluding the largest cluster for $p < p_c$. From this figure, we obtained $\gamma \simeq 2.38$, $p_c^{\rm eff} = 0.7560$, and $R \simeq 305$. For the data obtained excluding the largest cluster for $p < p_c$, we would obtain $\gamma \simeq 2.22$, $p_c^{\rm eff} = 0.7602$, and $R \simeq 360$. Clearly the data without excluding the largest cluster for $p < p_c$ yield much better result for γ (cf. $\gamma = \frac{43}{18}$ [19]) and the value of $p_c^{\rm eff}$ is also closer to the true p_c. From these results, one can expect that the data without excluding the largest cluster for $p < p_c$ would yield better estimates of physical quantities.

3. Cluster size distribution

Another, perhaps more significant, source of errors for the continuum models of *volumetric* inclusions is the definition of n_s inconsistent with the lattice counterpart. To see this clearly, let $n_s = N_s/N'$, where N_s is the number of clusters of size s. For lattice models, N' is the total number of sites, i.e., for d-dimensional cubic lattice, $N' = L^d$. For continuum models, researchers have chosen N' to be the total number of inclusions [10,13,15]. With this latter definition, N' is not a constant and depends on the concentration of inclusions for a given system, unlike the case for lattice percolation model.

The correct analogy for continuum models can be obtained by considering the probability that any site be-

longs to a finite cluster $\sum_s{}' n_s s$. Since $\sum_s{}' n_s s = p$ for $p < p_c$ and since $p = \eta$ $(= \frac{N}{V} V_1)$, it is natural to choose $N' = \frac{V}{V_1}$. Here N' can be considered as the "effective" total number of sites that a system of volume V can include.

We found by numerical investigation that the amplitude ratio estimated using this definition was considerably smaller than that obtained by a conventional choice for n_s. We also found that the amplitude ratio for the 2D PCS model with $L \geq 300$, estimated in this way, was close to the error bounds quoted for the lattice value, as we will see later.

4. Boundary conditions

The different boundary conditions employed in the simulation might also yield different estimates of R. As tests, we calculated χ using both free and periodic boundary conditions for selected cases of both the PCS and the RBP models and found that the two boundary conditions yielded different values of R. While data for periodic boundary conditions yielded slopes very close to the known lattice value of γ, those from free boundary conditions showed slightly larger values. Similar behavior was also observed for lattice percolation. To see this clearly, we carried out simulations for regular site percolation on a square lattice with $L = 2000$. Figure 2 shows the Monte Carlo data obtained using both free and periodic boundary conditions. The largest cluster was excluded only above p_c. The dotted and dashed lines for each set of data are the best fits, which show the same power law below and above p_c. The estimates for $(\gamma, p_c^{\text{eff}}, R)$ are (2.56,0.5955,231) and (2.39,0.5929,191) for free and periodic boundary conditions, respectively. In general, the data from free boundary conditions exhibited much larger statistical fluctuations and yielded a slope somewhat larger than the known value of γ. This suggests that periodic boundary conditions would yield better estimates of R.

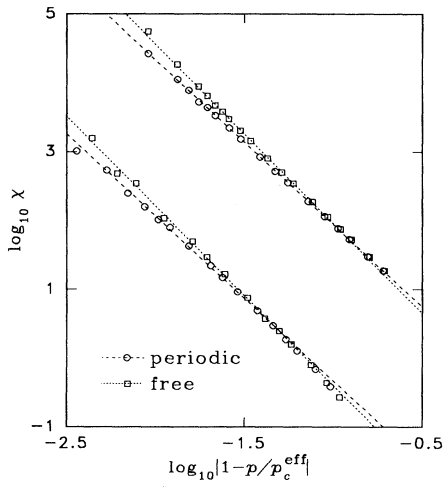

FIG. 2. Monte Carlo data of χ for ordinary site percolation on a square lattice of $L = 2000$, obtained using the free boundary condition (squares) and periodic boundary condition (circles), plotted on a double-logarithmic scale. The dotted lines are the power-law fit through the data for free boundaries and the dashed lines for periodic boundaries. The linear regression fitting on the same region shows that the periodic boundary condition yields a better estimate of γ.

III. RESULTS AND DISCUSSIONS

Since the main purpose of this work is to investigate the ratio of amplitudes for percolation susceptibilities below and above p_c for off-lattice models, we have calculated the susceptibilities, reducing errors in all possible ways as discussed in the preceding section. We first present the results for R for various size systems. We then present different analyses to confirm our estimates.

A. Continuum percolation of the PCS model

We have carried out Monte Carlo simulations for continuum percolation of the PCS model for selected values of λ, $\lambda = 0.3$, 0.5, and 0.8 in two dimensions and $\lambda = 0.6$ and 0.95 in three dimensions. The susceptibility χ was calculated for selected values of p, $0.0024 \leq |p - p_c| \leq 0.24$, and for various values of L, $50 \leq L \leq 300$ in two dimensions and $L = 20$, 30, 40, and 50 in three dimensions, both with and without excluding the largest cluster. For each of these cases, results were averaged over 50–5000 realizations, depending on p and L.

For the analysis, we first determined the approximate value of p_c^{eff} using the data excluding the largest cluster both below and above p_c. We then selected the data with the largest cluster below p_c^{eff} and without the largest cluster above p_c^{eff} to estimate R from the power-law fit. The power-law fits along the data points were made in a usual way: p_c was set as a parameter and the same power-law below and above p_c was assumed. It should be noted, however, that if one shifts the fitting region slightly toward or away from p_c, the slope and the displacement between the power law fits below and above p_c would vary appreciably. Since the amplitude ratio is obtained from the displacement, it would also vary depending on the choice of the fitting regions. In order to observe the size effect on R accurately, we have selected the fitting regions in such a way that the slope of the power-law fit yields the value close to the known lattice value of γ, $\gamma = \frac{43}{18} \simeq 2.39$ [19], and the fitting region is wide enough to determine R. This is certainly a reasonable choice since we are investigating whether or not R is different from the lattice value for percolation models for which the critical exponents are known to be the same.

In Fig. 3 we plotted, for the sake of comparison, the Monte Carlo data of χ in a double-logarithmic scale for two typical values of L, $L = 50$ and 300, for the 2D PCS model with $\lambda = 0.8$. The best power-law fit yielded $p_c = 0.7609$ and $\gamma = 2.40 \pm 0.02$ for $L = 50$ and $p_c = 0.7549$

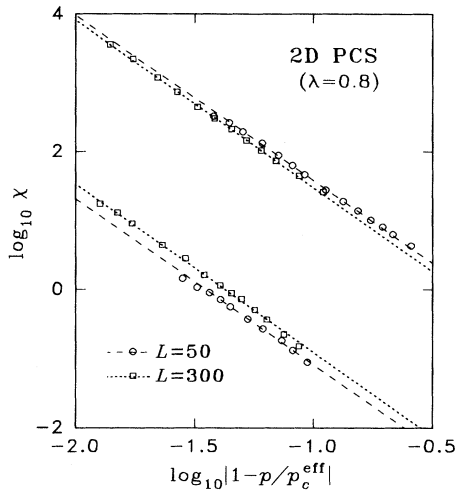

FIG. 3. Monte Carlo data of χ for the 2D PCS model with $\lambda = 0.8$ obtained for two typical values of L, using periodic boundaries. The amplitude ratio clearly depends on the size of system.

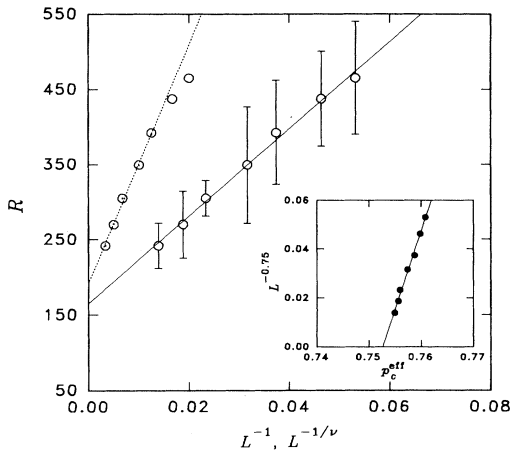

FIG. 4. Estimates of R plotted against L^{-1} (points without error bar) and against $L^{-1/\nu}$ (points with error bar) for the 2D model. The solid line is the regression fit along the data plotted against $L^{-1/\nu}$ and the dotted line along the data for $L \geq 80$ against L^{-1}. The inset is the plot of p_c^{eff} against $L^{-1/\nu}$, indicating the true $p_c \simeq 0.753$.

and $\gamma = 2.43 \pm 0.03$ for $L = 300$. With these estimates, we found that the Monte Carlo data exhibited a good power-law behavior in the wide region of $|p - p_c|$, implying that the exponent γ for the PCS model is indeed close to the lattice value. One important finding from the plot is that the amplitudes of χ below and above p_c are different for the two cases of L. This difference, although it appears not to be significant in the plot, affects R by a factor of nearly 2. For $L = 50$, we obtained $R = 465 \pm 75$, which is considerably larger than the lattice value $R = 196 \pm 40$ [20]. It should be noted, however, that this value is smaller, by a factor larger than 2, than the previous estimate [10]. We believe that this difference is due to the different definitions of n_s. For $L = 300$, on the other hand, we obtained $R = 242 \pm 30$, which is rather close to the lattice value but is slightly out of the error bounds. Results are summarized in Table I, together with those for other values of L. Clearly the estimates of amplitude ratio decrease as the size of the system increases.

Since analytically R is defined for an infinite system, one must carry out extrapolation, with the knowledge of how R scales as a function of L. Unfortunately, such information is not available to date. The easiest way one can visualize how R converges as $L \to \infty$ is to plot $R(L)$ against L^{-1} and estimate the intercept on the ordinate. However, in such an analysis, it would be rather difficult to extract R_∞ if R versus L^{-1} is not linear. Another possibility is to write from the scaling form $\chi(p, L) = L^{\gamma/\nu} f(|p - p_c| L^{1/\nu})$ that R should scale as a function of $L^{-1/\nu}$ as

$$R(L) = R_\infty (1 + aL^{-1/\nu} + \cdots) \tag{4}$$

(see the Appendix). Thus, plotting $R(L)$ against $L^{-1/\nu}$, one expects a linear behavior.

Figure 4 shows our estimates of R versus $L^{-1/\nu}$. Data without the error bars are plotted against L^{-1} while those with error bars against $L^{-1/\nu}$. The inset is the plot of p_c^{eff} against $L^{-1/\nu}$, in a way similar to that of renormalization calculations [21], and the true p_c is obtained as $p_c \simeq 0.753$, as expected [10]. Data plotted as a function of $L^{-1/\nu}$ appear to show a linear behavior, indicating that R indeed scales as in Eq. (4). From the plot, we estimate that $R_\infty = 170 \pm 50$, which falls within the error bounds of the lattice value. If, on the other hand, we consider the data against L^{-1}, those of $L \geq 80$ also appear to show a linear behavior, yielding $R \approx 190$, which is even closer to the lattice value (dotted line in the figure). These results ensure us that the amplitude ratio of susceptibilities for PCS model is similar to the lattice value.

The best known lattice value of R, on the other hand, was obtained by Monte Carlo simulation on a 4000×4000 square lattice, without the size effect being taken into account [20]. Since the size of system is relatively large, one might expect finite-size effects to be negligible in that work. However, if one measures R for different size systems, one would still be able to observe a decreasing trend as the size of system increases. In addition, the slope of the power-law fit was estimated to be about 2.36 in [20],

TABLE I. Estimates of p_c^{eff}, slope γ, amplitudes below and above p_c, and R from power-law fits for continuum percolation of the PCS model with $\lambda = 0.8$ in two dimensions.

L	p_c^{eff}	γ	$10C_-$	$10^4 C_+$	R
50	0.7608	2.40	1.534 ± 0.066	3.298 ± 0.335	465 ± 75
80	0.7586	2.38	1.517 ± 0.074	3.889 ± 0.408	390 ± 67
150	0.7560	2.38	1.396 ± 0.035	4.576 ± 0.220	305 ± 24
200	0.7557	2.40	1.289 ± 0.034	4.757 ± 0.493	271 ± 39
300	0.7549	2.43	1.112 ± 0.046	4.600 ± 0.339	242 ± 30

which is smaller by about 1.3% than the known lattice value. If one shifts the fitting region slightly away from p_c, one would obtain a slope closer to the known value of γ, but, in such a case, R would become slightly smaller. In our investigation on a square lattice of $L = 200$–2000, R appears to be about 180, with the error being similar to that quoted in [20] (not shown). This value of R agrees with that obtained from series extrapolation [22] and is also close to our estimate for the PCS model, thus indicating a universal behavior for R.

For other values of λ, $\lambda = 0.3$ and 0.5, the size effect appears not to be as significant as for the case $\lambda = 0.8$. Plotted in Fig. 5 are our data for $\lambda = 0.5$ and 0.3, obtained for $L = 80$. The power-law fits were obtained for $p_c^{\rm eff} = 0.8540$ and 0.9830 for $\lambda = 0.5$ and 0.3, respectively. Clearly data for the two cases exhibit different amplitudes, but the amplitude ratio appears to be similar. We believe this to be a good indication that the amplitude ratio is a universal quantity, while the amplitudes are not. For different size systems, data are not very different from that for $L = 80$. For example, when $\lambda = 0.5$, the values of R were estimated as $R = 201 \pm 41$, 192 ± 30, and 200 ± 26 for $L = 80$, 150 and 200, respectively; the slopes were estimated to be about 2.41 for all cases. Considering the errors, these values are similar to one another and are also consistent with the lattice value, again indicating a universal behavior of R.

Interestingly, as λ increases, the size effect appears to be more significant. Our data for $\lambda = 0.9$ and $L = 80$ yielded $R \simeq 420$, which is larger than the corresponding value for $\lambda = 0.8$. Unfortunately, we were not able to obtain data for larger systems because of the difficulty in generating equilibrium realizations due to too many rejections of moves by hard core overlaps; however, we believe that R would behave similarly to the case for $\lambda = 0.8$.

We have also carried out simulations for the 3D PCS model for selected values of λ, $\lambda = 0.6$ and 0.95. Results

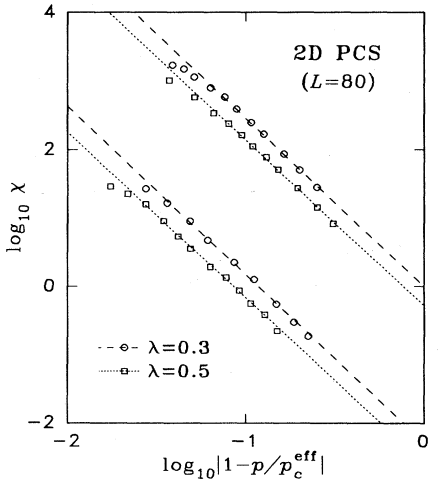

FIG. 5. Same as in Fig. 3, but for the 2D PCS model with $\lambda = 0.3$ and 0.5 for $L = 80$. The amplitude ratio appears to be similar for two cases, while the amplitudes are different.

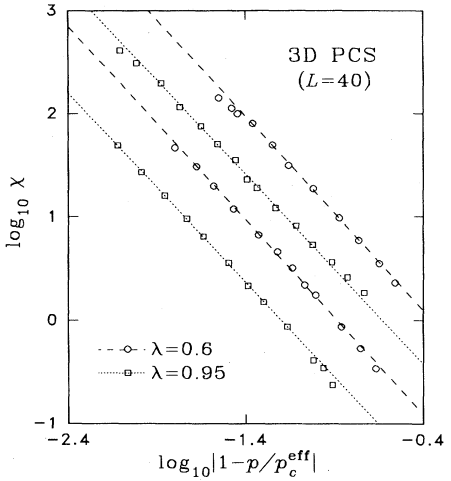

FIG. 6. Monte Carlo data of χ for the 3D PCS model for two typical values of λ (0.6 and 0.95) both with $L = 40$. The amplitude ratio obtained are close to the lattice value $R \simeq 11$.

were qualitatively similar to those for two dimensions. As the size of system increased, the amplitude ratio decreased slightly; however, the decreasing rate was not as significant as in two dimensions. Figure 6 shows the Monte Carlo data for $L = 40$ for both cases of λ. Again the amplitude ratio appears to be similar for two cases and is also consistent with the lattice value $R \simeq 8$–11 within errors [20], although the amplitudes themselves are different. This again supports our observation that the amplitude ratio is similar to the lattice value.

B. Randomly bonded percolation model

We have also carried out Monte Carlo simulations for off-lattice, randomly bonded percolation for selected values of μ, $\mu = 0.3$ and 0.5, for both two and three dimensions. The inclusion density selected are $\rho = 10$ for $\mu = 0.3$ and $\rho = 5$ for $\mu = 0.2$ for both dimensions. (Note that, for $\mu = 0.3$ and $L = 200$ in two dimensions, we used 4×10^5 random sites, which is equivalent to the number of occupied sites at p_c on a 821×821 square lattice.) The susceptibility was then calculated for various size systems, $16 \leq L \leq 200$ in two dimensions and $L = 10$, 15 and 20 in three dimensions, and the results were averaged over 50–2000 realizations, depending on the values of L and p. It should be noted that the parameters of our simulations for $\mu = 0.3$ in two dimensions are identical to those in Ref. [12], but we believe that our statistics are at least one order in magnitude better.

Figure 7 shows our Monte Carlo data for χ in two dimensions, plotted in a double-logarithmic scale, for two selected values of L, $L = 16$ and $L = 200$. The parameters used are $\mu = 0.3$ and $\rho = 10$, with the cutoff probability set for $r_c/\sqrt{\mu} = 8$ as in Ref. [12], and periodic boundary conditions were employed. The dashed and dotted lines in the plot are the best power-law fits. The estimates of γ and $p_c^{\rm eff}$ are $\gamma \simeq 2.44$ and $p_c^{\rm eff} = 0.1913$

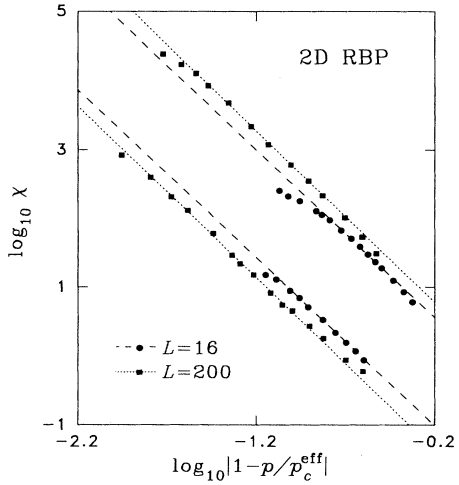

FIG. 7. Percolation susceptibilities for the 2D RBP model for $\mu = 0.3$, for two typical values of L. The displacement of the power-law fits below and above p_c are very different for two cases, indicating that the amplitude ratio for RBP model strongly depends upon the size of system.

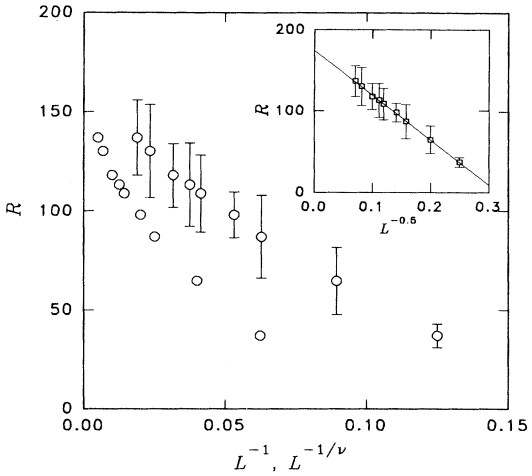

FIG. 8. Estimates of R plotted against L^{-1} (points without error bar) and against $L^{-1/\nu}$ (points with error bar) for the 2D RBP model. The inset is the plot of R against $L^{-1/2}$, yielding the best fit.

for $L = 16$ and $\gamma \simeq 2.49$ and $p_c^{\rm eff} = 0.1998$ for $L = 200$.

The amplitude ratio again appears to depend on the size of the system with R increasing as the size of the system increases. For $L = 16$, we estimate $R = 37 \pm 6$, which is one order of magnitude smaller than the lattice value, while for $L = 200$, we obtained a considerably larger value $R = 137 \pm 19$. Our estimate of R for $L = 200$ is of the same order of magnitude as the lattice value, although smaller by about 30%. Moreover, considering that the value of γ for $L = 200$ is slightly larger than the known lattice value, we expect R even larger than this value if we shift the fitting region toward p_c so that the slope of the power-law fit is similar to the known lattice value of γ. For example, if we select the region where $\gamma \simeq 2.39$, we would get $R \simeq 150$, which falls within the bounds of the lattice value, but the fitting region would be narrower. Simulations were also carried out for other values of L and we found that such an increasing trend of R as L increases was consistently observed for all selected values of L. Results are summarized in Table II.

In order to estimate R_∞ in the thermodynamic limit, we have plotted $R(L)$ against L^{-1} and $L^{-1/\nu}$, as for the 2D PCS model. Such plots are shown in Fig. 8; the points without error bar are plotted against L^{-1} and those with error bar against $L^{-1/\nu}$. Clearly R increases as the size of system increases and, if we make a simple eyeball extrapolation to the $L \to \infty$ limit, we get R about 160; however, neither of the plots seems to yield a linear behavior.

In order to extract a better estimate of R_∞, we have assumed that $R(L)$ scales as L^{-x}, where x is a parameter. As shown in the inset of Fig. 8, we found that $R(L)$ exhibited a good linear behavior for $x = 0.5$. Estimating from the figure, we obtained $R_\infty = 175 \pm 40$. This value of R is very close to our estimate for the PCS model in two dimensions and is also close to the lattice value, indicating that R for the RBP model is also similar to the lattice value. We, however, do not have any analytic argument of why R scales as $L^{-1/2}$, except the numerical investigation. One possible way to understand this result is to assume that both the leading and next leading terms in Eq. (5) might be non-negligible and the combination of the two terms might have resulted in such behavior. However, because the errors in our estimates of R are so large, we can still fit the data for $L \geq 70$ to get $R \simeq 170$.

Our data in Fig. 8 were obtained using the same parameters as those in the previous work [12]; however, our conclusions are totally different. These different conclusions are due to the two major differences between our work and the previous work. First, in the previous work, the data for various size systems were plotted on the same graph and the power-law fit was taken through all data, while in our work, we estimated $R(L)$ for each given size and the extrapolation to the $L \to \infty$ limit has been made to estimate R_∞. We have discussed the importance of the finite-size effect in Sec. I and our motivation was in fact to investigate such a size effect on R, which may have been ignored in the previous work. Second, we employed periodic boundary conditions, while free boundary con-

TABLE II. Estimates of $p_c^{\rm eff}$, slope γ, amplitudes below and above p_c, and R from power-law fits for the RBP model with $\mu = 0.3$ and $\rho = 0.3$ in two dimensions.

L	$p_c^{\rm eff}$	slope	C_-	$10^2 C_+$	R
16	0.1913	2.44	1.177 ± 0.142	3.164 ± 0.188	37 ± 6
25	0.1957	2.47	1.431 ± 0.171	2.250 ± 0.253	65 ± 17
50	0.1984	2.39	1.975 ± 0.145	2.015 ± 0.079	98 ± 12
80	0.1988	2.45	1.893 ± 0.161	4.672 ± 0.141	113 ± 21
150	0.1996	2.42	2.327 ± 0.270	1.787 ± 0.096	130 ± 23
200	0.1998	2.49	1.915 ± 0.101	1.399 ± 0.105	137 ± 19

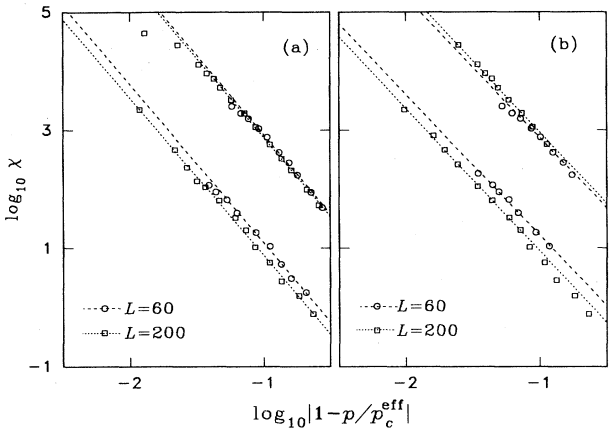

FIG. 9. Monte Carlo data for the 2D RBP model with $\mu = 0.3$ and $\rho = 10$, for two different size systems, obtained using free boundary conditions: (a) represents the best power fit and (b) is the plot drawn intentionally so that the slope is close to the known lattice value. Both plots appear to suggest that the amplitude ratio depends on the size of system.

ditions were used in the previous work.

In order to see how the boundary conditions affect the value of R, we repeated the same simulation using free boundary conditions. Figure 9 shows the data for two different size systems, $L = 60$ and 200: (a) is the best fit, which yields a wide region of power law, and (b) is the fit made intentionally so that the slope is close to the known lattice value of γ. (Note that the largest cluster was again excluded only above p_c.) For both cases, data clearly exhibit the size effect. In (a), the power-law fit yielded slopes of about 2.67 for both cases, indicating that the free boundary conditions indeed yield the exponent γ significantly overestimated from the best power-law fit, as we claimed in Sec. II. The estimates of amplitude ratio are $R \simeq 40$ for $L = 16$ and $R \simeq 120$ for $L = 200$, the latter of which is again considerably larger than the previous estimate [12]. If we choose the fitting region closer to p_c, we would be able to make the slope closer to the known lattice value, as shown in (b); however, the fitting region would be too narrow in this case. Even for such a plot, we found that R for $L = 200$ was an order of 100, in contrast to the value of 14 in the previous work.

One interesting point we should mention is that the data obtained excluding the largest cluster below and above p_c yield the slope close to the known lattice value

TABLE III. Same as Table II, but for the RBP model with $\mu = 0.2$ and $\rho = 5$ in two dimensions.

L	p_c^{eff}	slope	C_-	$10^2 C_+$	R
50	1.0410	2.40	5.016 ± 0.817	6.559 ± 0.583	76 ± 21
60	1.0511	2.43	5.430 ± 0.699	5.701 ± 0.329	95 ± 19
80	1.0520	2.40	5.865 ± 0.742	5.642 ± 0.267	104 ± 19
100	1.0578	2.44	6.031 ± 0.753	5.026 ± 0.190	119 ± 20
150	1.0611	2.40	6.899 ± 0.557	5.084 ± 0.260	136 ± 19

of γ, but still the amplitude ratio appears to depend on the size of the system. Estimates of R are $R \simeq 43$ ($p_c^{\text{eff}} = 0.2072$, $\gamma = 2.44$) for $L = 60$ and $R \simeq 127$ ($p_c^{\text{eff}} = 0.2043$, $\gamma = 2.42$) for $L = 200$, the latter of which is similar to our earlier estimate for the same size system but with periodic boundary condition. Thus, even for free boundary conditions, our data suggest that the amplitude ratio for the RBP model is close to the lattice value, indicating a strong universality between the RBP model and the lattice percolation model.

For $\mu = 0.2$, we have chosen $\rho = 5$, i.e., half as many particles as for $\mu = 0.3$, to reduce the computing time and the cutoff probability was set for $r_c/\sqrt{\mu} = 6$. Results were found to be qualitatively similar to those for $\mu = 0.3$, but the value of p_c^{eff} was significantly larger. The estimates are summarized in Table III. The amplitude ratio again depends on the size of system and, in the $L \to \infty$ limit, R_∞ would be within the bounds of the error for the lattice value, again suggesting a universal behavior for amplitude ratio.

So far, we have presented our simulation results for the RBP model only in two dimensions. In order to see if similar behavior is observable for the 3D RBP model as well, we carried out simulations in three dimensions using the same parameters for μ and ρ as in two dimensions. For $\mu = 0.2$ and $\rho = 5$, the amplitude ratio does not appear to strongly depend on the size of system. For $L = 10$ and 20, our estimates of R were identical within the errors (see Fig. 10) and were found to yield $R \simeq 10$, which is again similar to the lattice value in three dimensions. However, for $\mu = 0.3$ and $\rho = 10$, we obtained somewhat smaller values for R: $R \simeq 5.0$, 5.3, and 6.0 for $L = 10$, 15, and 20, respectively. If we make a simple extrapolation to the $L \to \infty$ limit with these data alone, we would still get R_∞ considerably smaller than the known lattice value. In order to derive a definite conclusion, however, we believe that more data for much larger sys-

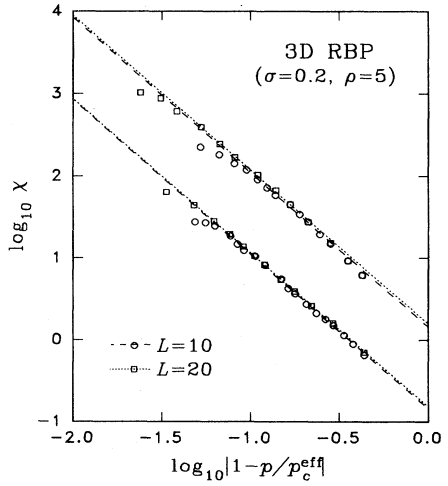

FIG. 10. Monte Carlo data for the 3D RBP model with $\mu = 0.2$ and $\rho = 5$, for two typical values of L. The amplitude ratio for both cases appears to be close to the lattice value.

tems are necessary. Unfortunately, such calculations are not currently possible because of prohibitively long computing time. However, considering the increasing trend of R against L and also the results for $\mu = 0.2$, we believe that a similar conclusion would be obtained for this case also.

C. Subtleties of finite-size scaling

In the previous two subsections we have shown that the size of system strongly affects the amplitude of susceptibilities for selected cases of continuum percolation of the PCS model and the RBP model. We have also shown by direct extrapolation that, as the size of system increases, the values of R converge to the lattice value for both models. In many instances, researchers alternatively employ the finite-size scaling analysis of $\chi(p, L)$ to estimate the infinite system results of R. However, our observation indicates some subtleties on the scaling analysis of susceptibilities.

For given L and p, the susceptibility $\chi(p, L)$ can be written, using the usual scaling argument, as

$$\chi_{\pm}(p, L) = |p - p_c|^{-\gamma} g_{\pm}(L/\xi) = L^{\gamma/\nu} f_{\pm}(L^{1/\nu}|p - p_c|), \quad (5)$$

where

$$f_{\pm}(x) = \begin{cases} \text{const} & \text{for } x \ll 1 \\ x^{-\gamma} & \text{for } x \gg 1. \end{cases} \quad (6)$$

Here ξ is the percolation correlation length, which diverges as $\xi \sim |p - p_c|^{-\nu}$ as $p \to p_c$, and the subscript $\pm$ implies above and below p_c. Thus, plotting the scaled susceptibility $\chi_{\pm}(p, L)/L^{\gamma/\nu}$ against a scaled variable $x \equiv L^{1/\nu}|p - p_c|$, one would get the data for various size systems collapsing onto a single curve [1]. However, this proposed scaling relation does not yield the correct asymptotic value of R if the amplitude ratio depends on the size of the system.

Suppose we have a double-logarithmic plot of $\chi_{\pm}(p, L)$ against $|p - p_c|$, as in Figs. 3 and 7. Then the scaling implies that, by shifting the plots by appropriate amounts, both horizontally and vertically, data for various size systems overlap one onto another, with the slope and the displacement of the power-law fit remaining unchanged for a given L. However, as we have seen, since the amplitude ratio (and alternatively the displacement of the power-law fits) depends on L for small L, it is, in principle, not possible to have all data for various L's on a single curve for small-size systems.

In order to confirm this observation numerically, one should determine what value of p_c should be used in Eq. (5). There are basically two choices. First, one can use the true p_c, if available. However, since p_c is not known accurately for most continuum percolation models, one can set p_c as a parameter and select the best value that shows a good power-law behavior and good data collapsing. Second, assuming that the power-law behavior of ξ depends on the size of system L as $\xi \propto |p - p_c^{\text{eff}}(L)|^{-\nu}$, one can argue that $p_c^{\text{eff}}(L)$ should be used for p_c. The first choice does not yield the same power-law behavior below and above p_c. Since for any (relatively small) finite L the power law with $\gamma = \gamma'$ holds only for $p_c^{\text{eff}}(L)$, data for various size systems are expected to split, without yielding a correct power-law behavior, if the true p_c is used. The second choice yields the correct power-law behavior for each given L; however, since the amplitude ratio depends upon the size of system L, data again are expected to split. Thus, in any case, one cannot expect the data to collapse onto a single curve for the entire region of p. (This does not imply a breakdown of scaling since scaling is, in principle, expected to hold in the vicinity of thermodynamic limit where $L \gg 1$.)

Figure 11 shows the finite-size scaling plot of the data for the 2D PCS model: (a) was obtained using the true p_c, i.e., $p_c = 0.7533$ [23] and (b) using $p_c = 0.7550$, for which the best power-law behavior and data collapsing occurred. In both cases, $\nu = \frac{4}{3}$ and $\gamma = \frac{43}{18}$ have been used [19]. The plot in (a) shows reasonably good data collapsing for various size systems; however, it does not yield the same power-law behavior below and above p_c, as we discussed before. The reader may also notice that data are about to split in the large x region for $p > p_c$ (lower plot). In (b), data also show fairly good collapsing, indicating that the quality of data collapsing is not sensitive to the choice of p_c. Although the plot shows the correct power-law behavior, the amplitude ratio estimate from this plot gives the wrong result. The solid lines are the best power-law fits one can draw; however, they are identical to those for the data for $L = 300$ in Fig. 3. This implies that one would most likely get an estimate of R similar to that of the largest system one used if one estimates R from the finite-size scaling plot, ignoring the size dependence of R.

For the RBP model, the situation is worse than that of the PCS model. Figure 12 shows the scaling function for the RBP model: (a) for true p_c, i.e., $p_c = 0.2005$ and (b) for $p_c^{\text{eff}}(L)$. (We have obtained the value of p_c

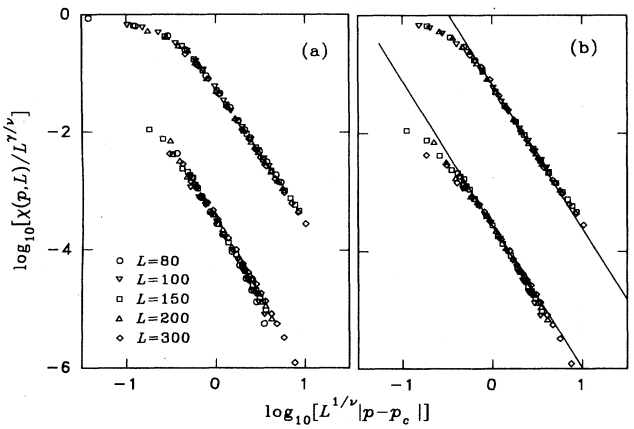

FIG. 11. Scaling function of Eq. (5) for the 2D PCS model with $\lambda = 0.8$, using (a) $p_c = 0.7533$ and (b) $p_c = 0.7550$. The solid lines in (b) are the shifted power-law fits of Fig. 3 for $L = 200$.

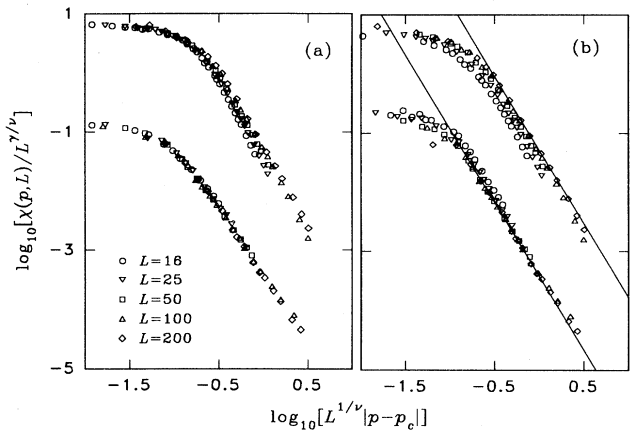

FIG. 12. Scaling function of Eq. (5) for the 2D RBP model with $\mu = 0.3$ and $\rho = 10$, using (a) true p_c, i.e., $p_c = 0.2005$, and (b) $p_c^{\text{eff}}(L)$. The solid lines in (b) are the best power-law fits for $L = 200$.

in a way similar to the inset of Fig. 3.) In (a), data for $p > p_c$ (lower plot) scale fairly well over the entire region of x. On the other hand, for $p < p_c$ (upper plot), data show two distinct regions. For small x (i.e., close to p_c), where the finite-size effect is the most prominent, data yield the correct asymptotic behavior and also show good collapsing. However, for the $x \gg 1$ region (where the power-law behavior is expected), data deviate, indicating that the scaling region is relatively narrow for the RBP model. As the size of system increases, the slope of each plot appears to change gradually and the plot tends to be more and more parallel to those of $p > p_c$. We expect that Monte Carlo data eventually yield correct power-law behavior if the system is sufficiently large so that the finite-size effect is negligible. In (b), although data for each given size system appear to yield the correct power-law behavior, those for various values of L do not collapse onto a single curve. The plot, however, shows a clear size dependence for the amplitude ratio. As the size of system increases, the displacement of the power-law fits also increases. The solid lines in the figure are the power-law fits for $L = 200$ that yield $R \simeq 137$, and we expect that R_∞ is even larger than this value, as discussed earlier.

We have also tested the scaling of the Monte Carlo data with other values of p_c, but we were not able to observe the correct power-law behavior simultaneously with the data collapsing. Thus, for both the PCS model and the RBP model, it is not possible to estimate R_∞ from the finite-size scaling plots of susceptibility functions.

IV. SUMMARY AND CONCLUSIONS

We have studied the amplitude ratio of percolation susceptibilities for two off-lattice models, the continuum percolation of the PCS model and the RBP model, where for both models the amplitude ratio was reported to be different from the lattice value while the various critical exponents remain unchanged. We found that the size of system significantly affects the estimates of amplitude ratio for selected cases of both models, particularly in two dimensions. For any finite system, the estimates of R were found to be significantly different from the known lattice values. However, as the size of system increases, R was found to converge to the lattice value for both models, indicating a "strong" universality between lattice and continuum percolation models. We thus believe that our work, together with the previous work [15], resolves the problem arising from the peculiar results of the amplitude ratio previously reported for the susceptibilities of continuum percolation models.

We also realize that there are other lattice models for which similar behavior has also been reported. These include the kinetic gelation model with random initiators [24] and the AB percolation model [25].

For the kinetic gelation model, Monte Carlo data on 30^3, 42^3, and 60^3 lattice sites indicated that the critical exponents ν and γ are slightly larger than those for ordinary lattice percolation, but R was found to be considerably smaller. Based on the estimate of R, the authors claimed a new universality for this model [24], although they later referred to their own work as an example similar to the RBP model. The amplitude ratio was estimated from the Monte Carlo data for three different values of L plotted on the same graph and the result was confirmed by the finite-size scaling analysis. However, as we discussed before, since the finite-size data collapsing implicitly assumes R being independent of the size of system, we believe that a more careful analysis is necessary to derive a definite conclusion for this model. At the same time, we also do not rule out the possibility that this model belongs to a new universality class. A signal of such behavior can be seen from the results for the backbone. While the fractal dimension of the backbone of ordinary lattice percolation is about 1.74, that for kinetic gelation was found to be about 2.22 [26]. Since the fractal dimension is related to the critical exponents via $d_f = d - \beta/\nu$, this implies that at least one of the critical exponents is different for the two models. If this is indeed the case, the critical exponents of kinetic gelation model may happen to be close enough so that the difference cannot be determined within errors by a numerical calculation, while that of the amplitude ratios is larger and more easily detectable.

For AB percolation, on the other hand, R was calculated on a triangular lattice of four different lattice sizes, $L = 1000$, 2500, 5000, and 10 000 and the average was reported as $R = 139 \pm 24$. Since this value already overlaps the errors with the lattice value, it is not clear whether or not R is different from the lattice value, even without the finite-size effect carefully taken into account. In addition, since the result $R = 145$ for $L = 10\,000$ in [25] is larger than the average of four lattice sizes, it is clear that the estimate of R increases as the size of system increases. Considering such a trend, we expect R to be larger than the reported value if the results are extrapolated to the $L \to \infty$ limit. We therefore cannot rule out a possible universal behavior of R, in the strong sense, between the

ordinary lattice and AB percolation models.

We have also discussed the subtleties of finite-size scaling for percolation susceptibilities. Our Monte Carlo data for the PCS model yielded fairly good data collapsing for the known value of p_c; however, the estimates of R from the finite size scaling do not appear to yield the value in the thermodynamic limit. For the RBP model, on the other hand, the scaling region appears to be relatively narrow and it was not possible to estimate the correct value of R from the finite-size scaling plot. However, the plots indicated a clear size dependence in R for both cases.

ACKNOWLEDGMENTS

The author is grateful to Professor H. Nakanishi for useful discussions, to Professor Titus for his critical reading of the manuscript, and to Purdue University Physics Department for the hospitality during his visit, during which part of this work was completed. The major part of this work was supported by Korea Research Foundation (administered by Ministry of Education, Korea Government) and also by Korea Science and Engineering Foundation under Grant No. 941-0200-035-2. The author is grateful for this support. He also acknowledges the partial support by the Basic Science Research Institution (Grant No. BSRI 95-2405) at Kyungpook National University.

APPENDIX: AMPLITUDE RATIO AS A FUNCTION OF L

From Eq. (3), the amplitude of susceptibility for a system of size L can be written as

$$C_{\pm}(L) = \chi_{\pm}(p, L)|p - p_c|^{\gamma}. \tag{A1}$$

Substituting Eq. (5) in (A1), one can write the amplitude $C_{\pm}(L)$ as a function of a scaled variable $x \equiv L^{1/\nu}|p-p_c|$, with the two extreme limits given as

$$C_{\pm}(x) = \begin{cases} x^{\gamma}, & x \ll 1 \\ C_{\pm,\infty}, & x \gg 1. \end{cases} \tag{A2}$$

Here $C_{\pm,\infty}$ is the amplitude above and below p_c in the $L \to \infty$ limit. Assuming that $C(x)$ is an analytic function of x^{-1}, it is easy to show that

$$R(L) = \frac{C_-(x)}{C_+(x)} = R_{\infty}\left(1 + \frac{a}{x} + \frac{b}{x^2} + \cdots\right). \tag{A3}$$

Since the amplitude ratio can be measured for the same values of $|p - p_c|$ below and above p_c, the leading correction term of $R(L)$ would be of $L^{-1/\nu}$, thus yielding Eq. (4).

[1] D. Stauffer and A. Aharony, *Introduction to Percolation Theory* (Taylor and Francis, London 1992).
[2] J. W. Essam, Rep. Prog. Phys. **43**, 833 (1980).
[3] S. Kirkpatrick, Rev. Mod. Phys. **45**, 574 (1973).
[4] E. T. Gawlinski and H. E. Stanley, J. Phys. A **14**, L291 (1981).
[5] B. Lorenz, I. Orgzall, and H.-O. Heuer, J. Phys. A **26**, 4711 (1993).
[6] A. Geiger and H. E. Stanley, Phys. Rev. Lett. **49**, 1895 (1982).
[7] W. J. Frith and R. Buscall, J. Chem. Phys. **95**, 5983 (1991).
[8] J. Kertesz and T. Vicsek, Z. Phys. B **45**, 345 (1982).
[9] T. Vicsek and J. Kertesz, J. Phys. A **14**, L31 (1980).
[10] S. B. Lee and S. Torquato, Phys. Rev. A **41**, 5338 (1990).
[11] For lattice percolation models, R was proven to be universal by field theoretical calculations; see, e.g., A. Aharony, Phys. Rev. B **22**, 400 (1980).
[12] D. Y. Kim, D. P. Landau, and H. J. Herrmann, Phys. Rev. B **35**, 3661 (1987).
[13] I. Balberg, Phys. Rev. B **37**, 2391 (1988).
[14] S. Torquato, J. Chem. Phys. **81**, 5079 (1984); **83**, 4776 (1985); **84**, 6345 (1986).
[15] S. B. Lee, Phys. Rev. B **42**, 4877 (1990).
[16] N. Metropolis, A. W. Rosenbluth, M. N. Rodenbluth, A. H. Teller, and E. Teller, J. Chem. Phys. **21** 1087 (1953); see also W. W. Woods, in *Physics of Simple Liquids*, edited by H. N. V. Temperly (North-Holland, Amsterdam, 1968).
[17] J. Hoshen and R. Kopelman, Phys. Rev. B **14**, 3438 (1976).
[18] H. Nakanishi and H. E. Stanley, Phys. Rev. B **22**, 2466 (1980).
[19] B. Nienhuis, Phys. Rev. Lett. **49**, 1062 (1982).
[20] J. Hoshen, D. Stauffer, G. H. Bishop, R. J. Harrison, and G. D. Quinn, J. Phys. A **12**, 1285 (1979).
[21] P. J. Reynolds, H. E. Stanley, and W. Klein, Phys. Rev. B **21**, 1223 (1980).
[22] W. F. Wolff and D. Stauffer, Z. Phys. B **29**, 67 (1978).
[23] From the plot of inset in Fig. 3, we obtained $p_c \simeq 0.753$. For Monte Carlo renormalization calculations, see, e.g., Ref. [10].
[24] H. J. Herrmann, D. P. Landau, and D. Stauffer, Phys. Rev. Lett. **49**, 412 (1982).
[25] H. Nakanishi, J. Phys. A **20**, 6075 (1987).
[26] A. Chhabra, D. P. Landau, and H. J. Herrmann, in *Fractals in Physics*, edited by L. Pietronero and E. Tossati (North-Holland, Amsterdam 1986); also see D. Stauffer, A. Coniglio, and A. Adams, Adv. Polym. Sci. **44**, 103 (1982).